Proceedings of the 21st ICSMGE, Vienna, Austria, 14 – 19 June 2026. Pistrol, Adam & Schweiger (eds.)
Published by: ÖGG, Austrian Society for Geomechanics, Salzburg, Austria, ISBN 978-3-9503898-4-5
https://doi.org/10.53243/ICSMGE2026-2396

Characteristics of transport paths of water vapor inside unsaturated sandy ground during evaporation from bare soil

Yuta Jikuya, Motoyuki Suzuki
Graduate School of Sciences and Technology for Innovation, Yamaguchi University, Ube, Yamaguchi, Japan, yuta-j@yamaguchi-u.ac.jp

ABSTRACT: To quantify the moisture variability in the soil after a rainfall event, it is essential to comprehend the amount of evaporation from the ground surface. In the present study, the authors propose a method for estimating the ground surface evaporation from general meteorological data by the bulk method. In this method, the unsaturated evaporation properties (the relation between the moisture content and the molecular diffusion distance) must be obtained in advance, depending on the soil conditions, such as the soil type and compaction. Although functional equations for the unsaturated evaporation properties have been empirically proposed, their predictability for unknown soil conditions is insufficient. A mathematical model to estimate the unsaturated evaporation properties from the fundamental physical quantities of the soil (hereafter, the evaporation property model) will be developed herein. The evaporation property model is a model for bare surface soil. It evaluates the path of water vapor as it is transported from the water surface in the void to the ground surface, considering the void structures in the soil. Then, the characteristics of the number of water vapor paths, a parameter in the model, will be considered based on the unsaturated evaporation properties obtained from laboratory experiments using sandy soil.

KEYWORDS: Evaporation, evaporation efficiency, bulk method, unsaturated sandy soil.

1 INTRODUCTION

In recent years, rainfall-induced slope failures have become increasingly severe, highlighting the urgent need for effective countermeasures. Since it is impractical to implement structural countermeasures, such as constructing slope failure prevention facilities on all hazardous slopes, there is a growing demand for enhancing non-structural countermeasures. These include the development of evacuation and warning systems. Warnings, such as natural disaster warnings and traffic restrictions, are issued primarily based on rainfall intensity (e.g., Sugiyama et al., 1995). However, clear criteria for canceling these warnings after a rainfall event has ceased are often lacking.

Slope stability generally improves after a rainfall event as the soil moisture content decreases over time. Therefore, the amount of evaporation from the ground surface can serve as an essential indicator when determining the appropriate timing of warning cancellations. The bulk method (Kondo, 1994) enables the estimation of ground surface evaporation solely from general meteorological data and the ground surface temperature by clarifying the ease of evaporation (evaporation efficiency) depending on the local soil properties. Although various models for evaporation efficiency have been proposed (Deardorff, 1978; Barton, 1979; Kondo et al., 1990; Lee & Pielke, 1992), these models are empirical and exhibit limited predictive capability for previously untested soil types.

This study focuses on the empirical parameter known as the molecular diffusion distance, which represents the unsaturated evaporation properties used in Kondo's (1990) evaporation efficiency model. A mathematical model is developed here to estimate the molecular diffusion distance using fundamental physical quantities of the soil (hereafter, the evaporation property model). Furthermore, the characteristics of the number of water vapor paths, a parameter in the model, are experimentally examined using several types of sandy soil with different grain size characteristics. Additionally, the relationship between the number of water vapor paths and unsaturated seepage properties is examined.

2 UNSATURATED EVAPORATION PROPERTIES

The evaporation properties in unsaturated soil are evaluated by the evaporation efficiency, which is a fundamental parameter of the bulk method. Evaporation efficiency β is a dimensionless quantity that expresses the ease with which evaporation from the ground surface occurs; it has a value between 0 and 1.0 depending on the moisture content (e.g., β = 0 under dry conditions and β = 1.0 under saturated conditions). Figure 1 illustrates the relationship between the volumetric water content (VWC) and the evaporation efficiency, as determined from experiments conducted by Kondo et al. (1990). As shown in the figure, the evaporation efficiency function can be divided into two trends after a certain moisture content: I) β values at an almost constant 1.0, and II) β values that begin to decrease from 1.0 and approach 0 as the moisture content decreases. In Range I, where the moisture content is relatively high, the ground surface evaporation is controlled by the atmospheric moisture demand. On the other hand, in Range II, where the moisture content is low, the ground surface evaporation is less than the atmospheric moisture demand due to the restrictions of the soil. The boundary moisture content (VWC = 0.3 in Figure 1), which determines the trend in the evaporation efficiency function, is influenced by the soil conditions, such as soil type and compaction (Kondo & Motoyama, 1994). The solid and dashed lines in the figure represent the calculation results of the evaporation efficiency model proposed by Kondo et al. (1990), hereafter referred to as the Kondo model, as follows:

$$\beta = \left[1 + g_a F(\theta) / D_{atm}\right]^{-1} \tag{1}$$

where g_a is the exchange speed (primarily a function of wind speed) and D_{atm} is the molecular diffusion coefficient for water

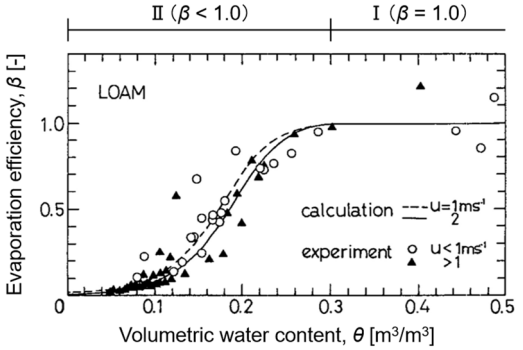

Figure 1. Relationship between VWC and evaporation efficiency for loam obtained by Kondo et al. (1990) (corrected with additions).

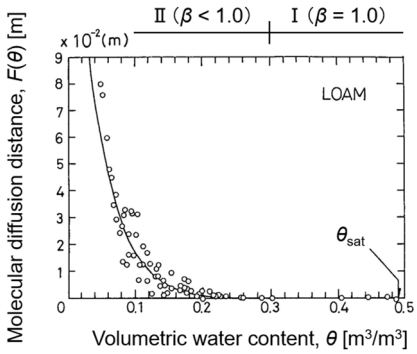

Figure 2. Relationship between VWC and molecular diffusion distance for loam obtained by Kondo et al. (1990) (corrected with additions).

Table 1. $F(\theta)$ constants for representative soil types (Source: Kondo, 1994).

Soil type	F_1 [m]	F_2	θ_{sat}
Loam	2.16×10^2	10.0	0.490
Sand	8.32×10^5	16.6	0.392
Fine sand	7.00×10^3	11.2	0.397

vapor (Camillo et al., 1983). Moreover, the Kondo model introduces a resistance function ($F(\theta)$: molecular diffusion distance [m]), which depends on the VWC of the shallow uppermost soil layer (Figure 2). The solid line in the figure represents the following empirical relationship:

$$F(\theta) = F_1(\theta_{sat} - \theta)^{F_2} \tag{2}$$

The constants (F_1, F_2, θ_{sat}) in Equation (2) are proposed for the representative soil types, as listed in Table 1. Parameter $F(\theta)$ represents the effective transport distance for water vapor from the water menisci within the soil voids to the ground surface, i.e., the length of the transport paths of water vapor. As shown in Figure 2, it is inversely related to β. Since g_a and D_{atm} in Equation (1) can be determined from meteorological data and the ground surface temperature alone, identifying a suitable expression for $F(\theta)$ that reflects the local soil properties is crucial for accurately estimating β.

3 EVAPORATION PROPERTY MODEL

3.1 *Kita-Sako model*

Building upon the fundamental concept of the Kita-Sako model (Sako & Kitamura, 2006), a mathematical model is proposed to estimate the molecular diffusion distance, $F(\theta)$. The Elementary Particulate Body (EPB), shown in Figure 3, is considered in the Kita-Sako model; it consists of a small cluster of soil particles. The EPB is modeled by the Elementary Particle Model (EPM), shown in Figure 4. The voids in the EPB are modeled as a pipe with a diameter D_v and an inclination angle γ, while the soil particles in the EPB are modeled as the other impermeable parts. The height of the EPM, DH, is empirically assumed to be the same length as the grain size at 10% passing by mass, D_{10}, and the depth of the EPM is equal to D_v. Therefore, the volume of

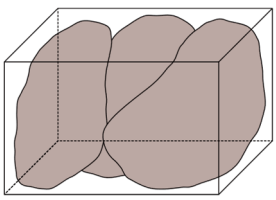

Figure 3. Elementary Particulate Body (EPB).

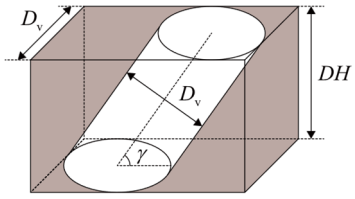

Figure 4. Elementary Particle Model (EPM).

the EPM, V_e, and that of the pipe in the EPM, V_p, can be expressed as follows:

$$V_e = D_v \cdot \left(\frac{D_v}{\sin\gamma} + \frac{DH}{\tan\gamma} \right) \cdot DH \tag{3}$$

$$V_p = \pi \cdot \left(\frac{D_v}{2} \right)^2 \cdot \frac{DH}{\sin\gamma} \tag{4}$$

Soil is a natural material composed of particles with complex shapes and sizes, resulting in irregular geometries for both the solid and void phases. The Kita-Sako model accounts for this irregularity by adopting pipe diameter D_v and inclination angle γ as random variables. The probability density functions for D_v, $P_d(D_v)$, and γ, $P_c(\gamma)$, are introduced to describe the distributions of these variables, as shown in Equations (5) and (6).

$$P_d(D_v) = \frac{1}{\sqrt{2\pi} \cdot \zeta_v \cdot D_v} \cdot \exp\left[-\frac{(\ln D_v - \lambda_v)^2}{2 \cdot \zeta_v^2} \right] \tag{5}$$

$$P_c(\gamma) = \begin{cases} \dfrac{2/\pi - 2 \cdot \zeta_c}{\pi/2} \cdot \gamma + \dfrac{2}{\pi} - \zeta_c & -\dfrac{\pi}{2} \le \gamma \le 0 \\ -\dfrac{2/\pi - 2 \cdot \zeta_c}{\pi/2} \cdot \gamma + \dfrac{2}{\pi} - \zeta_c & 0 \le \gamma \le \dfrac{\pi}{2} \end{cases} \tag{6}$$

where λ_v is the mean value of $\ln D_v$, ζ_v is the standard deviation of $\ln D_v$, and ζ_c is the distribution parameter which describes the pentagonal shape (= 0.159).

3.2 *Modeling of transport paths of water vapor*

Considering a bare uppermost soil layer with a unit area and empirical depth of 0.02 m (Kondo et al., 1990), the transport paths of water vapor during the evaporation process are modeled. The evaporation path in the soil (Figure 5(a)) is modeled as a cylindrical pipe with a diameter D_p and a height F_i (Figure 5(b)). Here, subscript i is used to distinguish the multiple evaporation paths present in the soil. In the Kita-Sako model, capillary action in unsaturated soils is taken into consideration by assuming that the voids drain in order from the largest to the most minor diameters. Therefore, if d represents the maximum diameter of the voids filled with water,

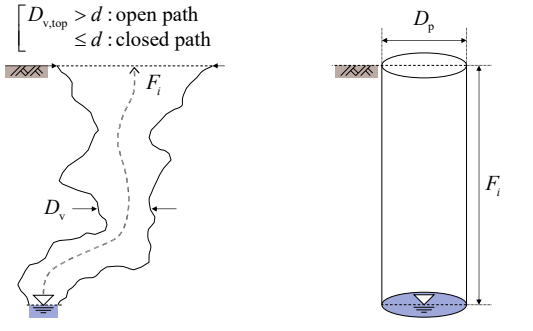

(a) Evaporation path (b) Model cylindrical pipe

Figure 5. Modeling of evaporation path.

the evaporation paths can have diameters in the range of d to ∞, following $P_d(D_v)$. Based on this assumption, the diameter D_p of the model cylindrical pipe is defined as the mean diameter of the voids D_v over this range, as expressed in Equations (7) and (8).

$$D_p = \int_d^{\infty} D_v \cdot P_d(D_v) / (1 - CDF)\, dD_v \tag{7}$$

$$CDF = \int_0^{d} P_d(D_v)\, dD_v \tag{8}$$

where the CDF is the cumulative distribution function and represents the probability that a void is filled with water. Furthermore, assuming no volume change during the modeling process, the height F_i of the model cylindrical pipe is equivalent to the length of the evaporation path. Considering the void size $D_{v,top}$ at adjacent to the uppermost part of the evaporation path (i.e., closest to the ground surface), the path is either open to the atmosphere with $D_{v,top} > d$, according to a probability of (1 - CDF), or closed within the soil with $D_{v,top} \leq d$, according to a probability of CDF. At this point, a new parameter, the number of water vapor paths, N_p, is introduced, and it is assumed that there are only N_p paths connected to the atmosphere (effective paths). By assuming that the total air volume in the soil, V_a (Equation (9)), contributes to the formation of effective paths in proportion to the probability of (1 - CDF), an air volume equilibrium (Equation (10)) can be established.

$$V_a = \int_d^{\infty} \int_{-\frac{\pi}{2}}^{\frac{\pi}{2}} \frac{V_p}{V_e - V_p} \cdot P_d(D_v) \cdot P_c(\gamma)\, d\gamma\, dD_v \times \frac{V}{1+e} \tag{9}$$

$$V_a \times (1 - CDF) = \frac{\pi}{4} \cdot D_p^{\,2} \times \sum_{i=1}^{N_p} F_i \tag{10}$$

where e is the void ratio and V is the total volume of soil. When an evaporation path is closed within the soil, evaporation occurs at the ground surface and the path length becomes 0 (i.e., it is considered an ineffective path). Therefore, molecular diffusion distance $F(\theta)$ is defined as the weighted mean of the ineffective path length (= 0) and the mean length of the effective paths, with the weights given by their respective probabilities, as expressed in the following equation:

$$\begin{aligned} F(\theta) &= \frac{1}{N_p} \cdot \sum_{i=1}^{N_p} F_i \times (1 - CDF) + 0 \times CDF \\ &= \left(\frac{\pi}{4} \cdot D_p^{\,2} \times N_p \right)^{-1} \cdot V_a \times (1 - CDF)^2 \end{aligned} \tag{11}$$

4 NUMBER OF WATER VAPOR PATHS

4.1 *Measurement conditions*

To obtain evaporation efficiency β and molecular diffusion distance $F(\theta)$ as functions of the VWC, laboratory evaporation tests were conducted following the method proposed by Jikuya et al. (2024). In addition, unsaturated seepage properties, which are known to depend on the void size, were measured using a HYPROP instrument (METER Group, Inc., USA), including the soil water characteristic curve (SWCC) and the hydraulic conductivity function (HCF). The HYPROP instrument employs the simplified evaporation method (Schindler, 1980). In both tests, measurements were taken at 30-minute intervals.

The tested soils included Toyoura sand, No. 5 silica sand, and No. 3 silica sand, all of which have relatively narrow grain size distributions, as well as Higashimata soil (a sample of volcanic sandy soil that passed through a 2-mm sieve), which has a wider grain size distribution. The physical properties of each soil and the measurement conditions are summarized in Table 2. The specimens for the laboratory evaporation tests were prepared to have a diameter of 126.5 mm and a height of 20 mm, targeting a relative density of 50% and an initial degree of saturation of 60%. The specimens used for the HYPROP instrument were prepared to have a diameter of 80 mm and a height of 50 mm. They were compacted to a target relative density of 50% and then infiltrated with degassed water for one day. By inputting the soil particle density, void ratio, and grain size distribution (GSD) into the Kita-Sako model, the continuous function of the GSD and the corresponding void size distribution (VSD) were calculated (Figure 6).

4.2 *Results and discussion*

Figure 7 shows the evaporation efficiency, molecular diffusion distance, and number of water vapor paths as functions of the VWC. The plots provided in Figure 7(a) and (b) are the results of the laboratory evaporation tests. Using these plots and the VSD calculated from the Kita-Sako model (Figure 6), Figure 7(c) was obtained by back-calculating Equation (11). The dashed line in Figure 7(b) represents the calculation results of the Kondo model (Equation (2)) for sand. Although all the

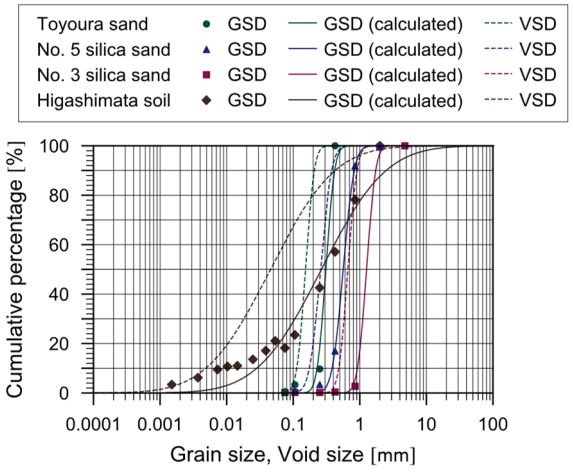

Figure 6. Grain size distribution (GSD) and void size distribution (VSD).

Table 2. Physical properties and measurement conditions.

		Grain size characteristic		Laboratory evaporation test		HYPROP instrument	
	Soil particle density	Mean grain size	Fine fraction content	Void ratio	Degree of saturation	Void ratio	Degree of saturation
	ρ_s [Mg/m^3]	D_{50} [mm]	F_c [%]	e	$S_{r,0}$ [%]	e	$S_{r,0}$ [%]
Toyoura sand	2.640	0.32	0.05	0.750	58.67	0.759	89.49
No. 5 silica sand	2.559	0.61	0.67	0.750	57.64	0.751	81.64
No. 3 silica sand	2.556	1.41	0.18	0.785	57.72	0.780	77.16
Higashimata soil	2.497	0.34	18.17	1.491	56.82	1.484	82.49

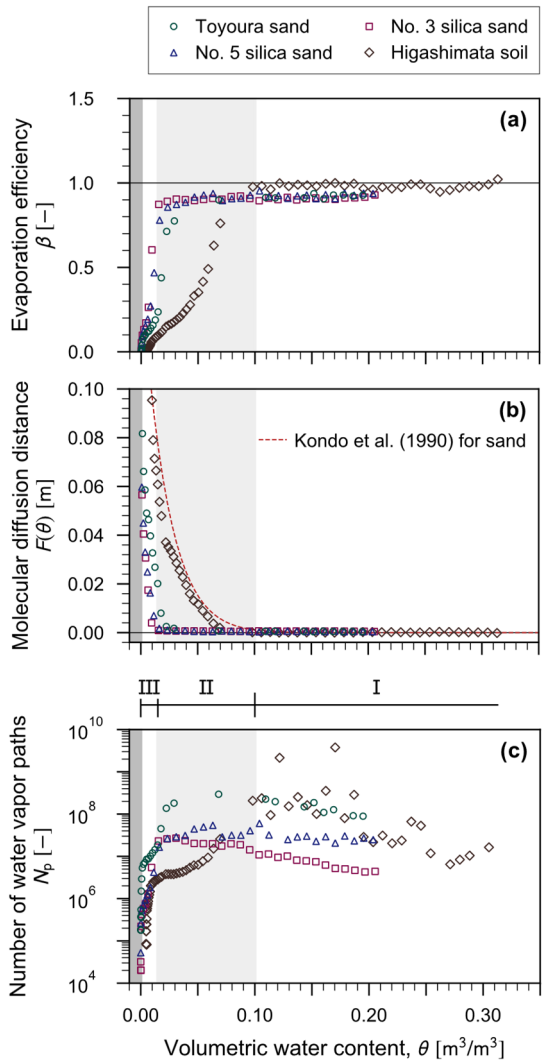

Figure 7. Evaporation efficiency, molecular diffusion distance, and number of water vapor paths in relation to volumetric water content.

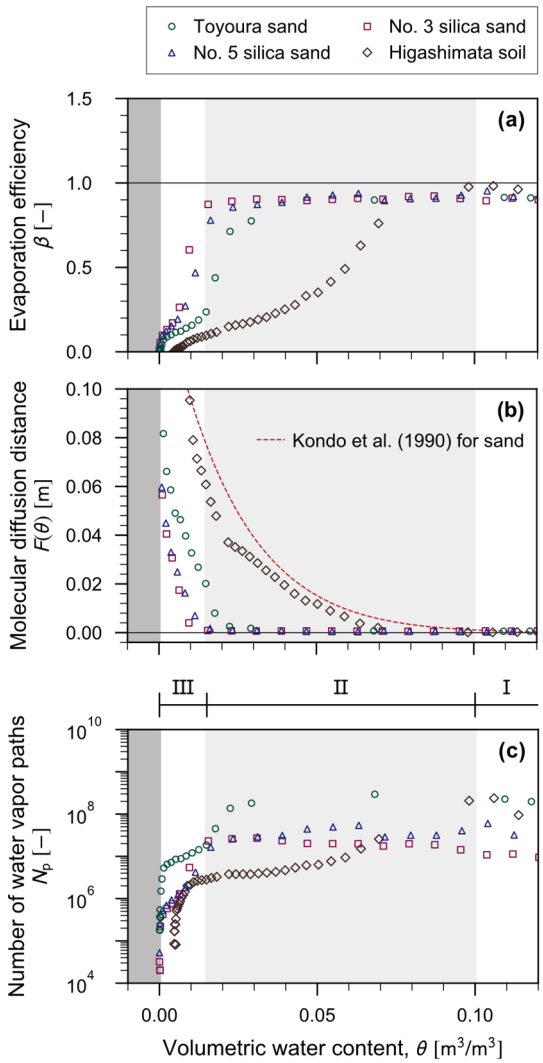

Figure 8. Evaporation efficiency, molecular diffusion distance, and number of water vapor paths in relation to volumetric water content (enlarged view of the low-moisture-content region in Figure 7).

soil samples used in this study are classified as sandy soil, the functional forms of $F(\theta)$ differ among them, and the Kondo model does not adequately capture these differences. Furthermore, the low-moisture-content region in Figure 7 is enlarged and given in Figure 8. From Figure 7(c) and Figure 8(c), it can be seen that the number of water vapor paths, N_p, changes with the decreasing VWC in the following three stages (each stage in the Higashimata soil is represented in the figures).

Stage I : The VWC decreases at approximately regular intervals, while N_p increases slowly.

Stage II : As evaporation progresses, the decrease in the VWC becomes suppressed, and N_p decreases.

Stage III : Eventually, the VWC hardly changes, and N_p decreases rapidly, converging to 1.

In the following paragraphs, the characteristics of N_p in each stage are discussed in relation to β and $F(\theta)$. In addition, the trend in N_p is discussed based on the SWCCs and HCFs measured by the HYPROP instrument shown in Figure 9 and Figure 10. It should be noted that, due to the performance limitations of the tensiometers used in the HYPROP instrument, data in the dry range could not be obtained, and HCF measurements could not be conducted until the hydraulic gradient exceeded the threshold value specified by Peters & Durner (2008). Therefore, in Figure 9, to obtain an overall tendency for the SWCC for Higashimata soil, additional data measured in the dry range using the WP4C instrument (METER Group, Inc., USA) are included. The WP4C instrument employs the chilled-mirror dew point technique (Gee, 1992). In this study, five specimens were prepared at each degree of saturation, ranging from 5% to 25% (in 5% increments), under a relative density of 50%, resulting in a total of 25 measurements. In addition, measurement data in the wet range for Toyoura sand reported in previous studies (Kono & Nishigaki, 1981; Kawanishi et al., 1987; Uno et al., 1990; Abe, 1994) are included in Figure 10 to provide an overall tendency for the HCF.

4.2.1 *Stage I*

At this stage, the β values are at an almost constant 1.0, and the ground surface evaporation follows the atmospheric moisture demand, which is influenced by factors such as temperature and humidity. Since the tests were conducted in a temperature-controlled room, with minimal fluctuations in temperature and humidity, the amounts of evaporation, indicated by the decrease in the VWC, are approximately equal for the specified time intervals. Additionally, since $F(\theta)$ is approximately 0, suggesting that the distance the water vapor moves during the evaporation process is extremely short, it can be inferred that evaporation mainly occurs in the capillary voids near the ground surface at this stage. The resultant increase in N_p is

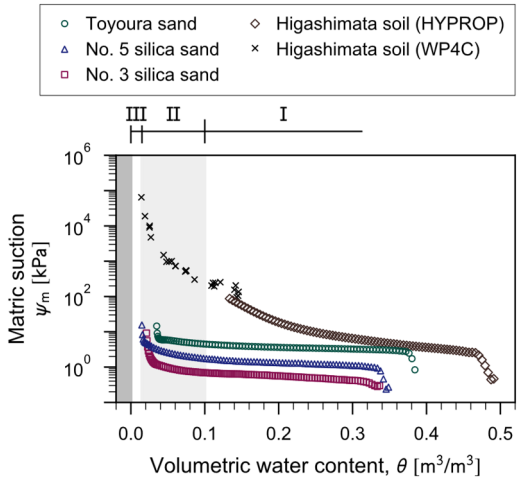

Figure 9. Soil water characteristic curves (SWCC).

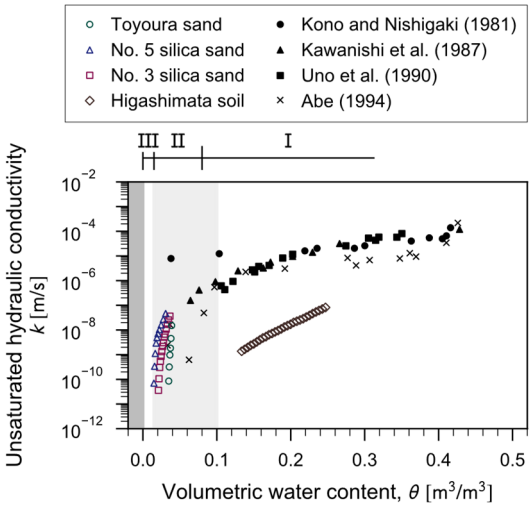

Figure 10. Hydraulic conductivity function (HCF).

thought to be due to the formation of voids near the ground surface, which occurs as evaporation progresses. For Toyoura sand, No. 5 silica sand, and No. 3 silica sand, which have narrow grain size distributions, N_p tends to have higher values as mean grain size D_{50} decreases, and the transition to *Stage II* slightly earlier. In contrast, for the sandy soil with a wider grain size distribution, Higashimata soil, *Stage II* transition occurs at a higher VWC compared to the samples with a narrower grain size distribution. It is noteworthy that the method used to calculate β in this study may underestimate it depending on the soil type (Jikuya et al., 2024), and there are differences in β between Higashimata soil and other soil samples. Since this difference affects the results of the N_p calculation, no comparison can be made of the values for N_p.

From the SWCCs shown in Figure 9, it is observed that, for Toyoura sand, No. 5 silica sand, and No. 3 silica sand, N_p tends to be higher with increasing matric suction. Furthermore, near the VWC corresponding to the transition to *Stage II*, the SWCCs rise sharply. Considering the significant change in the slope of the HCFs for Toyoura sand shown in Figure 10 (Zimmie & Riggs, 1981; Tuller & Or, 2001), this boundary moisture content corresponds to the residual VWC (Vanapalli et al., 1998). On the other hand, within the HCFs range measured in this study, no clear relationship was observed between the value of N_p and the unsaturated hydraulic conductivity.

4.2.2 *Stage II*

At this stage, β decreases rapidly from approximately 1.0. At the same time, as the VWC decreases, the ground surface evaporation gradually decreases due to soil restrictions. Furthermore, $F(\theta)$ increases from approximately 0, indicating that the distance the water vapor moves during the evaporation process becomes longer. This suggests that evaporation is occurring in the capillary voids located more deeply below the ground surface. Based on this, it can be interpreted that, as the evaporation paths elongate, previously isolated paths begin to confluence, leading to a decrease in N_p. This stage continues up to roughly the same VWC for Toyoura sand, No. 5 silica sand, and No. 3 silica sand, regardless of mean grain size D_{50}, and continues over a wide range up to a slightly higher VWC for Higashimata soil. However, no clear relationship was observed between the value of N_p and the grain size characteristics.

Since the SWCCs and HCFs in this stage are not sufficiently measured, it is necessary to complement the data by measuring the Toyoura sand, No. 5 silica sand, and No. 3 silica sand using the WP4C instrument.

4.2.3 *Stage III*

At this stage, β decreases to approximately 0, and $F(\theta)$ becomes significantly longer than the specimen height of 0.02 m. As a result, evaporation is minimal, and the VWC remains almost unchanged. Given the very low VWC, it is considered that pore water is held by strong adsorptive forces on the surfaces of the soil particles (Vanapalli et al., 1998). Furthermore, the sharp decrease in N_p suggests that the evaporation paths, which had continued confluence since *Stage II*, ultimately converge into a single, long, and highly tortuous path. This explains the immense value of $F(\theta)$, as evaporation must occur from pore water that is firmly held within complex and constricted paths. In Higashimata soil with a high fine fraction content, the VWC range corresponding to *Stage III* is broader, suggesting a higher quantity of adsorbed water. This observation is consistent with the findings of Kawabata et al. (2006), who reported that soils with a higher fine fraction content hold more adsorbed water.

As the VWC is extremely low in this stage, it is not easy to obtain reliable measurements of the SWCC and HCF. Therefore, new approaches, such as fitting to an unsaturated seepage model (e.g., Fayer & Simmons, 1995), should be considered for better characterization.

5 CONCLUSIONS

In this paper, the transport paths of water vapor during the evaporation process from bare soil were mathematically modeled to estimate the unsaturated evaporation properties from the fundamental physical soil properties. Furthermore, the characteristics of a newly introduced parameter, the number of water vapor paths, N_p, were investigated by back-calculating the results of laboratory evaporation tests using sandy soil. The main results of this paper are as follows:

1. A mechanistic and probabilistic model was developed to evaluate the molecular diffusion distance based on the void structures in soil.
2. The fundamental relationship between N_p and the moisture content was clarified to have three stages as the soil dries out: I) a slow increase, II) a decrease, and III) a rapid decrease and convergence to 1.
3. Sandy soils with a smaller mean grain size and a wider grain size distribution were found to have wetter soils transitioning to *Stage II*, characterized by a broader range in moisture content during this stage.
4. The moisture content at the boundary between *Stage I* and *Stage II* was found to correspond to the residual VWC.

In the present study, no clear relationship was identified between the value of N_p and the grain size characteristics or unsaturated seepage properties. For future considerations, further testing on a variety of soil types is needed.

6 ACKNOWLEDGEMENTS

This work was supported by JSPS KAKENHI Grant Number JP24K22976.

7 REFERENCES

Abe, H. 1994. An experimental study on evaluation method of mechanical properties of unsaturated soil. *The University of Tokyo Doctorial Dissertation*, 280. (in Japanese)

Barton, I.J. 1979. A parameterization of the evaporation from nonsaturated surfaces. *J. Appl. Meteor.* 18(1), 43-47.

Camillo, P.J., Gurney, R.J., and Schmugge, T.J. 1983. A soil and atmospheric boundary layer model for evapotranspiration and soil moisture studies. *Water Resour. Res.* 19(2), 371-380.

Deardorff, J.W. 1978. Efficient prediction of ground surface temperature and moisture, with inclusion of a layer of vegetation. *J. Geophys. Res.* 83(C4), 1889-1903.

Fayer, M.H., and Simmons, C.S. 1995. Modified soil water retention functions for all matric suctions. *Water Resour. Res.* 31(5), 1233-1238.

Gee, G.W., Campbell, M.D., Campbell, G.S., and Campbell, J.H. 1992. Rapid measurement of low soil water potentials using a water activity meter. *Soil Sci. Soc. Am. J.* 56, 1068-1070.

Jikuya, Y., Sako, K., and Ito, S. 2024. Study on the calculation method of evaporation efficiency in bulk method considering the difference in heat capacity between soil and water. *Japanese Journal of JSCE* 80(15), 23-15040. (in Japanese)

Kawabata, S., Ikeda, K., and Kamiya, M. 2006. Relationship between physical properties and frost-susceptibility of volcanic coarse-grained soils in Hokkaido. *Doboku Gakkai Ronbunshuu C* 62(1), 35-44. (in Japanese)

Kawanishi, M., Tanaka, Y., Komada, H., and Shiozaki, I. 1987. A fundamental study on characteristics of unsaturated seepage. *Proc. of the Symposium on Current Status of Research on Engineering Properties of Unsaturated Soils*, 245-252. (in Japanese)

Kondo, J. 1994. *Meteorology of the water environment, - water and heat balance of the earth -*. Japan: Asakura Publishing Co. Ltd., 194–198. (in Japanese)

Kondo, J., and Motoyama, K. 1994. An experiment on evaporation parameters of soil. *J. Japan Soc. Hydrol and Water Resour.* 7(5), 430-435. (in Japanese)

Kondo, J., Saigusa, N., and Sato, T. 1990. A parameterization of evaporation from bare soil surfaces. *J. Appl. Meteor.* 29(5), 385-389.

Kono, I., and Nishigaki, M. 1981. An experimental study on characteristics of seepage through unsaturated sandy soil. *Proc. of the Japan Society of Civil Engineers* 1981(307), 59-69. (in Japanese)

Lee, T.J., and Pielke, R.A. 1992. Estimating the soil surface specific humidity. *J. Appl. Meteor.* 31(5), 480-484.

Peters, A., and Durner, D, 2008. Simplified evaporation method for determining soil hydraulic properties. *J. Hydrol.* 356(1-2), 147-162.

Sako, K., and Kitamura, R. 2006. A practical numerical model for seepage behavior of unsaturated soil. *Soils and Foundations* 46(5), 595-604.

Schindler, U. 1980. Ein schnellverfahren zur messung der wasserleitfähigkeit im teilgesättigten boden an stechzylinderproben. *Arch. Acker- u. Pflanzenbau u. Bodenkd.*, Berlin, 24(1), 1-7. (in German)

Sugiyama, T., Okada, K., Muraishi, H., Noguchi, T., and Samizo, M. 1995. Statistical rainfall risk estimating method for a deep collapse of a cut slope. *Soils and Foundations* 35(4), 37-48.

Tuller, M., and Or, D. 2001. Hydraulic conductivity of variably saturated porous media: Film and corner flow in angular pore space. *Water Resour. Res.* 37(5), 1257-1276.

Uno, T., Sato, T., Sugii, T., and Tsuge, H. 1990. Method of test for permeability of unsaturated sandy soil with controlled air pressure. *Doboku Gakkai Ronbunshu* 1990(418), 115-124. (in Japanese)

Vanapalli, S.K., Sillers, W.S., and Fredlund, M.D. 1998. The meaning and relevance of residual state to unsaturated soils. *Proc. of the 51st Canadian Geotechnical Conference*, Edmonton, Canada, 4-7 October 1998.

Zimmie, T.F., and Riggs, C.O. 1981. *Permeability and groundwater contaminant transport*. United States: Am. Soc. Test. Mater., Spec. Tech. Publ., 168-181.